Finite-size and finite-time scaling for kinetic rough interfaces

Rahul Chhimpa and Avinash Chand Yadav [*]
Department of Physics, Institute of Science, Banaras Hindu University, Varanasi 221 005, India

(Received 19 October 2023; revised 16 February 2024; accepted 30 April 2024; published 29 May 2024)

We consider discrete models of kinetic rough interfaces that exhibit space-time scale invariance in height-height correlation. We use the generic scaling theory of Ramasco *et al.* [Phys. Rev. Lett. **84**, 2199 (2000)] to confirm that the dynamical structure factor of the height profile can uniquely characterize the underlying dynamics. We apply both finite-size and finite-time scaling methods that systematically allow an estimation of the critical exponents and the scaling functions, eventually establishing the universality class accurately. The finite-size scaling analysis offers an alternative way to characterize the anomalous rough interfaces. As an illustration, we investigate a class of self-organized interface models in random media with extremal dynamics. The isotropic version shows a faceted pattern and belongs to the same universality class (as shown numerically) as the Sneppen model (version A). We also examine an anisotropic version of the Sneppen model and suggest that the model belongs to the universality class of the tensionless Kardar-Parisi-Zhang (tKPZ) equation in one dimension.

DOI: 10.1103/PhysRevE.109.054130

I. INTRODUCTION

The phenomenon of *kinetic surface roughening* (a dynamically growing rough surface or interface) occurs in diverse contexts, and it has been a topic of much interest, particularly in nonequilibrium statistical physics, in advancing theoretical understanding [1–4]. Typical instances include fluid flow in porous media [5], the spreading of fracture cracks [6,7], and fungal growth [8]. In condensed matter physics, the study of the thin-film growth formed by particle deposition processes (for example, molecular-beam epitaxy [9–11]) seems important technologically.

Strikingly, many systems of kinetic surface roughening exhibit scaling features. Determining the universality class of the model has been a crucial aspect. A set of independent critical exponents characterizing the scaling properties of the rough surface determines the universality class. The most familiar classes are random deposition, Edwards-Wilkinson (EW) [12] and Kardar-Parisi-Zhang (KPZ) [13–19]. Several discrete surface roughening models have been introduced and examined in the past to uncover the underlying mechanisms. Random deposition with surface relaxation or growth preferred at local minima [20,21] represents a discrete model of the EW class, while several models (Eden [22], ballistic deposition [23], and restricted solid on solid [24]) belong to the KPZ class. The interface between turbulent phases in liquid crystal films [25,26] also falls into the KPZ class. Najem *et al*. [27] studied the morphology of urban skylines for which the roughness properties are commensurate with the EW and KPZ classes. Fujimoto *et al*. [28] examined the interface dynamics in the strongly interacting one-dimensional Bose gas and found that the high-filling case corresponds to the EW class.

While surface roughening remains one aspect, several other properties have been of concern. For example, the distribution of width [29], the maximal height [30], the density of extrema [31], the cycling effects [32], and the maximal spatial persistence [33].

Let $h(x,t)$ be the height profile of a fluctuating interface on a one-dimensional substrate with $1 \leqslant x \leqslant L$. The commonly used characterization of the height profile is the global interface width

$$w(t,L) = \langle \overline{[h(x,t) - \bar{h}(t)]^2} \rangle^{1/2}. \tag{1}$$

The overline in Eq. (1) represents the average over all sites x, and the angular brackets $\langle \cdot \rangle$ denote the ensemble average over different realizations. For the scale-invariant rough interface, the global interface width exhibits the Family-Vicsek dynamic scaling ansatz [23]

$$w(t,L) = t^{\chi/z} f[L/\xi(t)]. \tag{2}$$

The correlation length varies as $\xi(t) \sim t^{1/z}$, where z denotes the *dynamical exponent*. The scaling function $f(u)$ in Eq. (2) assumes a form

$$f(u) \sim \begin{cases} u^{\chi}, & u \ll 1, \\ \text{constant}, & u \gg 1, \end{cases} \tag{3}$$

where χ is the *roughness exponent* that characterizes the stationary regime $\xi(t) \gg L$. The *growth exponent* $\beta = \chi/z$ describes the short-time behavior of the interface.

In many growth models, it was found that while the local width (and height-height correlation) behave similarly to Eq. (2) as $w(t,l) = t^{\beta} f_l[l/\xi(t)]$ (measured in windows of size $l \ll L$), the scaling function differs from Eq. (3) as

$$f_l(u) \sim \begin{cases} u^{\chi_{\rm loc}}, & u \ll 1, \\ \text{constant}, & u \gg 1. \end{cases} \tag{4}$$

In Eq. (4), the local roughness exponent $\chi_{\rm loc}$ is an independent exponent [34,35]. This intriguing feature is the so-called

[*]Corresponding author: jnu.avinash@gmail.com

anomalous roughening and has been of much interest [36–39]. López suggested that the anomalous features emerge from the nontrivial dynamics of the mean square local slope $\langle\overline{(\nabla h)^2}\rangle \sim t^{2\kappa}$ with $\chi_{\rm loc} = \chi - z\kappa$ [34]. Recent studies showed anomalous behavior in a class of kinetic rough interfaces externally driven by long-time correlated noise [40–42].

Ramasco *et al.* [35] observed that a *generic scaling theory* for the structure factor can reveal the unique dynamical features, including the anomalous feature. However, to get data collapse for the dynamical structure factor, the exponents χ and z need to be known (discussed below). The scaling analysis of the global and local interface widths can provide an estimate of the two exponents and a sign of the existence of anomalous features, respectively. Alternatively, on a double logarithmic scale, the envelope and individual curve slopes for the dynamical structure factor can provide an approximate estimate of the roughness exponent χ and the *spectral roughness exponent* χ_s, respectively [43]. χ_s is a remarkable characteristic for understanding the broad subclass of the underlying process (discussed below). However, a precise estimate of the spectral roughness exponent remains missing. Moreover, a *systematic analysis* of the scaling feature of the dynamical structure factor seems lacking. Ramasco *et al.* [35] examined the Sneppen model (version A) [44], a self-organized interface depenning in random media, showing faceted patterns ($\chi_s > \chi$) with $\chi_s = 1.35$. Our analysis, well-supported numerically, reveals that the precise value of the exponent is $\chi_s = 3/2$.

In this paper, we employ systematically both *finite-size scaling* (FSS) and *finite-time scaling* (FTS) methods for the scaling analysis of the dynamical structure factor. A clean data collapse ensures a precise estimation of the independent critical exponents that eventually determine the universality class of the process. We examine a class of self-organized interface models in random media driven by *extremal dynamics* as discussed in Ref. [45]. Strikingly, the FSS of the structure factor provides an alternative description of the anomalous features. Interestingly, the isotropic version of the model displays anomalous features (a faceted pattern) and belongs to the same universality class as that of the Sneppen model. We also introduce and analyze an anisotropic variant of the Sneppen model and suggest the model belongs to the tKPZ universality class [46,47].

More recently, Fontaine *et al.* [48] explained the existence of one missing unstable fixed point (with the critical dynamical exponent $z = 1$) associated with the celebrated KPZ equation in one dimension. Basically, this is the limit of an infinite nonlinear coupling known as the tensionless (or inviscid limit) KPZ equation. In fact, there are three fixed points: one stable and two unstable. The stable fixed point corresponds to the KPZ class with $z = 3/2$. For zero nonlinearity, the KPZ equation reduces to the EW class ($z = 2$), which corresponds to the second unstable fixed point.

The organization of the paper is as follows. In Sec. II, we present the definition of the models describing rough interfaces evolving in random media with extremal dynamics. Section III provides the FSS and FTS methods for the dynamical structure factor. The numerical results obtained from simulations for FTS are presented in Sec. IV. Finally, the paper concludes with a brief discussion in Sec. V.

II. MODELS

Consider a one-dimensional lattice with site labels $1, 2, \ldots, L$, along with periodic boundary conditions. To each site, assign the interface height $h(x, t)$. The time is typically measured in monolayer units, the number of deposited particles per unit system size. We also use the same unit. The model-specific update rules are as follows.

A. Sneppen model (version A)

Sneppen [44] introduced a discrete model of the kinetic roughening interface in the presence of quenched disorder. The model is a striking example of a self-organized rough interface, showing scale invariance in the height profile. Initially, the interface is flat $h(x, t = 0) = 0$. To each site, assign a random pinning force $\eta[x, h(x)]$, drawn from a uniform distribution between 0 and 1. The update rules include the following steps. Choose a site x' with the smallest pinning force only among the sites that satisfy the following slope constraints (Kim-Kosterlitz conditions): $[|h(x) + 1 - h(x - 1)| \leqslant 1$ and $|h(x) + 1 - h(x + 1)| \leqslant 1]$. Then, increase the height of that site by one unit: $h(x') = h(x') + 1$.

The model produces a rough interface with a faceted pattern. The global width characteristic exponents are $z = 1$ and $\chi = 1$, implying that the process shows *self-similarity* [44]. Although the global interface width characteristic exponents seem trivial, the analysis of the dynamical structure factor revealed an unexpectedly nontrivial feature with $\chi_s > \chi$ [35].

B. Anisotropic Sneppen model (version A)

We also examine an anisotropic variant of the model. Here, we implement a different local constraint, $h(x + 1) - h(x) \geqslant 0$. The rest of the dynamical update occurs similarly, as mentioned for the Sneppen model. Eventually, the local slope can have $h(x + 1) - h(x) = -1$ or $\gg 1$. While the process keeps the two exponents $z = 1$ and $\chi = 1$ unchanged, the spectral roughness exponent becomes $\chi_s < \chi$ (intrinsically anomalous). Surprisingly, our analysis suggests that the model belongs to the tKPZ universality class.

As seen from Fig. 1, the height profile for the anisotropic case does not satisfy the space inversion symmetry ($x \to -x$). When the dynamics change from the isotropic to the anisotropic Sneppen model, a transition occurs from a subclass with a faceted pattern to a subclass with an intrinsic anomalous feature for the kinetic roughening interfaces. The lack of spatial inversion symmetry implies a change in the universality class.

C. Isotropic Maslov-Zhang model (version B)

Maslov and Zhang [45] introduced and solved a model of self-organized criticality with a preferred direction. The model is an anisotropic variant of the Zaitsev model [49]. They also suggested physically relevant interface dynamics in random media (quenched disorder) belonging to the same universality class. Our interest is in a variant of the roughening interface model.

In the isotropic version of the model, $F(x) = A[h(x + 1) - 2h(x) + h(x - 1)] + \eta[x, h(x)]$ determines the local force.

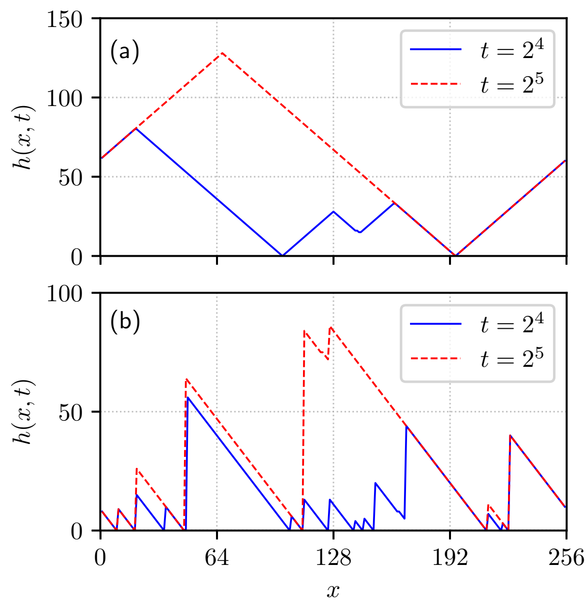

FIG. 1. For the Sneppen model, the typical height profiles at two values of time (in monolayers) with $L = 2^8$ for (a) isotropic and (b) anisotropic dynamical rules.

Here A is the relative strength of the elastic force, and $\eta[x, h(x)]$ is a random pinning strength drawn from a uniform distribution between 0 and 1. We use $A = 1$ in simulations. Initially, the interface is a groove: $h(x = 2i - 1, t = 0) = 1$ and $h(x = 2i, t = 0) = 0$, where $i = 1, 2, \ldots, L/2$. At each site, the slope is $h(x+1, t) - h(x, t) = \pm 1$. The local minimum occurs at the value $n_c(x) = h(x+1, t) - 2h(x, t) + h(x-1, t) = 2$. In general, n_c can be -2, 0, or 2. The update occurs as $h(x') = h(x') + 2$, where the site x' corresponds to the sites with $n_c = 2$ and having the largest value of the quenched disorder $\eta(x, h)$, or simply the maximum force location for $n_c(x) + \eta(x, h)$. We call it the Maslov-Zhang model (version B-1), or (MZB-1). As numerically shown below, the model belongs to the same universality class as the Sneppen model.

It is useful to emphasize that while the Sneppen model follows the slope constraints (Kim-Kosterlitz conditions), the MZB-1 model has the restrictions of the single-step (SS) model [50]. While the height in the SS model increases by 2 with probability p if $n_c(x) = 2$, it decreases by 2 with probability $1 - p$ if $n_c(x) = -2$. The SS model belongs to EW or KPZ for $p = 1/2$ or $p \neq 1/2$, respectively [51]. Interestingly, it is possible to obtain exact results for the SS model in one dimension since there exists a map with the kinetic Ising model [50,52] and the asymmetric simple exclusion process [53].

D. Maslov-Zhang model (version B)

In the anisotropic version of the model (say, MZB-2), the local driving force acting on a site x is $F(x) = A[h(x+1) - h(x)] + \eta[x, h(x)]$. We again use $A = 1$ and the same initial condition as mentioned for the isotropic version of the model. Only two height gradients, $h(x+1) - h(x) = \pm 1$, are possible. Updates occur similarly at a site where the force has maximum strength. The suggested exponents are $z = 1$ and $\chi = 1/2$ [45]. As shown below, the model does not exhibit anomalous features. However, the dynamical exponent takes a slightly different value.

III. SCALING ANALYSIS FOR STRUCTURE FACTOR

We devote this section to introducing the reader to the Ramasco *et al.* theory of generic kinetic surface roughening [35], which will be used in the rest of the paper to explain the numerical results. In terms of the Fourier transform of the height function, $\hat{h}(k, t) = L^{-1/2} \sum_x [h(x, t) - \bar{h}(t)] \exp(ikx)$, one can write an expression for the dynamical structure factor (or power spectrum) $S(k, t) = \langle \hat{h}(k, t)\hat{h}(-k, t)\rangle$. This also reveals the height-height correlation $G(l, t) = 4/L \sum_{2\pi \leqslant k \leqslant \pi/a_0} [1 - \cos(kl)] S(k, t) \propto \int_{2\pi/L}^{\pi/a_0} (dk/2\pi)[1 - \cos(kl)] S(k, t)$, where a_0 is the lattice spacing [35]. If we fix the time t, $\bar{h}(t)$ becomes constant, implying that the structure factor of h or $h - \bar{h}$ remains the same.

A. FSS for $S(k, N, L)$

For kinetic rough interfaces, the dynamical structure factor is typically a function of the growth time and the system size in the growth regime. To understand the detailed scaling features comprehensively, we apply both the FSS and FTS methods. We first show the results for the FSS for a fixed value of the growth time (in monolayers). The structure factor remains constant for the low-wave number regime and a power law $\sim 1/k^{2\chi_s+1}$ in the nontrivial regime. Interestingly, the structure factor remains independent of the system size, even for anomalous rough interfaces. We checked this numerically for rough interfaces belonging to different classes, for example, EW, KPZ, and the isotropic (or anisotropic) Sneppen model (cf. Fig. 2). If we only consider the growth time as the number of deposited particles N, the structure factor clearly depends on L even in the high wave-number regime for anomalous processes. Mathematically, one can interpret the system size-independent feature as

$$S(k, N, L) = S(k, t), \quad \text{with } t = N/L,$$

for fixed growth time (in monolayers). As t is constant, the structure factor is only a function of the wave number. If the spectral roughness exponent χ_s is different from the roughness exponent χ, the underlying process has an anomalous feature.

B. FTS for $S(k, t)$

Varying the time t in the growth regime, the structure factor $S(k, t)$ as a function of the wave number k shows typically two distinct regimes. Below a cutoff of $k \ll k_0 \sim L^{-1} \sim t^{-1/z}$, the power remains independent of k but increases with time as $\sim t^a$. In the nontrivial wave number regime $k \gg k_0$, the structure factor, in general, can show scaling in both arguments $\sim 1/k^{2\chi_s+1}$ and $\sim t^b$. Now, we can write an expression for the structure factor as a function of the two arguments (wave

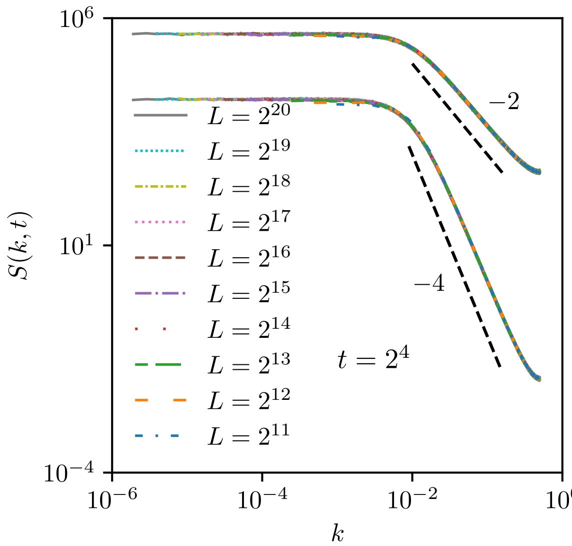

FIG. 2. The FSS of the structure factor for the Sneppen model, with the system sizes $L = 2^{11}, 2^{12}, \ldots, 2^{20}$. The lower (upper) curves correspond to the isotropic (anisotropic) update rule with the spectral roughness exponent $2\chi_s + 1 = 4$ (2). The dashed straight line guides the slope. Since $\chi_s \neq \chi = 1$, the rough interfaces are anomalous. The growth time (in monolayers) is $t = 2^4$. Each curve is ensemble averaged over a 2×10^3 independent realization of the rough interfaces.

number and time) [35,37]

$$S(k,t) \sim \begin{cases} t^a, & k \ll t^{-1/z}, \\ t^b/k^{2\chi_s+1}, & t^{-1/z} \ll k \ll 1/2. \end{cases} \tag{5}$$

As proposed in the previous studies, the structure factor shown in Eq. (5) (in one dimension) follows the scaling ansatz

$$S(k,t) = k^{-(2\chi+1)}G(kt^{1/z}) = t^{(2\chi+1)/z}H(u), \tag{6}$$

where the scaling functions in Eq. (6) are

$$G(u) \sim \begin{cases} u^{2\chi+1}, & \text{if} \quad u \ll 1, \\ u^{2(\chi-\chi_s)}, & \text{if} \quad u \gg 1, \end{cases} \tag{7a}$$

$$H(u) \sim \begin{cases} \text{constant}, & \text{if} \quad u \ll 1, \\ u^{-(2\chi_s+1)}, & \text{if} \quad u \gg 1. \end{cases} \tag{7b}$$

Since $G(u) = u^{2\chi+1}H(u)$, the two scaling functions are complementary. This implies that for one physical property $S(k,t)$, one scaling function suffices for its complete characterization.

Comparing Eqs. (5) and (6), it is easy to recognize the exponents a and b in terms of the conventional exponents z, χ, and χ_s as

$$a = (2\chi + 1)/z, \tag{8}$$

and

$$b = 2(\chi - \chi_s)/z. \tag{9}$$

Equation (8) also suggests the dynamical exponent satisfy a scaling relation

$$z = 1/(a - 2\beta).$$

Equation (9) also implies simple conditions for different subclasses [35]

$$b = 0 \Rightarrow \chi_s = \chi \quad \begin{cases} \text{if } \chi_s < 1 \Rightarrow & \text{Family Vicsek}, \\ \text{if } \chi_s > 1 \Rightarrow & \text{super rough}, \end{cases}$$

$$b > 0 \Rightarrow \chi_s < \chi \quad \Rightarrow \quad \text{intrinsic anomalous},$$

$$b < 0 \Rightarrow \chi_s > \chi \quad \Rightarrow \quad \text{faceted pattern}.$$

Notice that the time t considered here is such that the global interface width corresponds to the growth regime. It is easy to note that no trace of the spectral roughness exponent appears in the global width

$$w^2(t) = \int dk S(k,t) = t^{\frac{(2\chi+1)}{z}} \int H(u)\frac{d(kt^{1/z})}{t^{1/z}}$$
$$\sim t^{\frac{2\chi}{z}} \sim t^{2\beta}.$$

Because of this, the structure factor is the most relevant characterization and provides subtle details of the underlying process. Numerically, it is easy to determine the scaling function $H(u \sim kt^{1/z}) = t^{-a}S(k,t)$. We only require the two critical exponents a and $z = 1/(a - 2\beta)$. One can easily estimate the two exponents by examining the scaling behavior of the power in the low-wave number component and the square of the global interface width as a function of time. Replacing $t \to L^z$ in Eqs. (5) or (6), one can immediately obtain the global interface width as $w^2 \sim L^{2\chi}$, which consistently reflects the scaling behavior of the structure factor in the stationary regime.

IV. NUMERICAL RESULTS FOR FTS

Figures 3 and 4 display the properties of the dynamical structure factor and its analysis using FTS for the Sneppen model. Table I presents the estimated critical exponents. Similarly, we studied the MZB-1 and MZB-2 models. Clean data collapse excellently supports the numerically estimated exponents within the statistical error. Our results are consistent with Refs. [35,44] that suggest $z = 1$ and $\chi = 1$ for the Sneppen model. This implies that $a = (2\chi + 1)/z = 3$ and $2\beta = 2\chi/z = 2$. Further, our finer numerical results [cf. Fig. 3(b)] suggest $b = -1$. Eventually, the spectral roughness exponent is $\chi_s = \chi - bz/2 = 3/2$, which differs slightly from the previously estimated value of 1.35 [35]. We also get the same set of exponents for the MZB-1 model, indicating that the two models belong to the same universality class.

Similarly, the critical exponents for the anisotropic Sneppen model are $z = 1$, $\chi = 1$, and $\chi_s = 1/2$ (cf. Figs. 5 and 6), implying the model shows intrinsically anomalous behavior. More recently, Rodríguez-Fernández *et al.* [46] provided a direct numerical simulation of the tKPZ equation

$$\partial_t h = \frac{\lambda}{2}(\partial_x h)^2 + \eta(x,t), \tag{10}$$

which shows intrinsic anomalous behavior with $z = 1$, $\chi = 1$, and $\chi_s = 1/2$. Here, λ is the nonlinearity parameter, and $\eta(x,t)$ denotes uncorrelated Gaussian noise in space-time with zero mean. One can describe the space derivative of the height profile $u = \partial_x h$ by the inviscid stochastic Burger

TABLE I. A summary of the critical exponents characterizing the dynamical structure factor properties. For the Sneppen model, the first column presents the expected theoretical exponents.

Exponent		Sneppen model	[35]	MZB-1		Anisotropic Sneppen model	MZB-2
b	-1	$-0.98(1)$		$-1.00(1)$	1	0.99(1)	0
2β	2	1.98(1)		1.98(1)	2	1.96(1)	1.71(4)
$z = 1/(a - 2\beta)$	1	1.03(2)	1	1.01(2)	1	1.04(2)	0.59(4)
$\chi = \beta z$	1	1.02(3)	1	1.00(3)	1	1.02(3)	0.51(7)
$\chi_s = \chi - \frac{bz}{2}$	1.5	1.53(4)	1.35	1.50(4)	0.5	0.51(2)	0.51(7)

equation

$$\partial_t u = \lambda u \partial_x u + \partial_x \eta(x, t).$$

Assuming u as a rough interface, they examined its dynamical structure factor and found $z = 2/3$, $\chi = 1/3$, and $\chi_s = -1/2$. They also examined the stochastic Korteweg–de Vries (KdV) equation (an important model of weakly nonlinear waves)

$$\partial_t u = c\partial_x^3 u + u\partial_x u + \partial_x \eta(x, t),$$

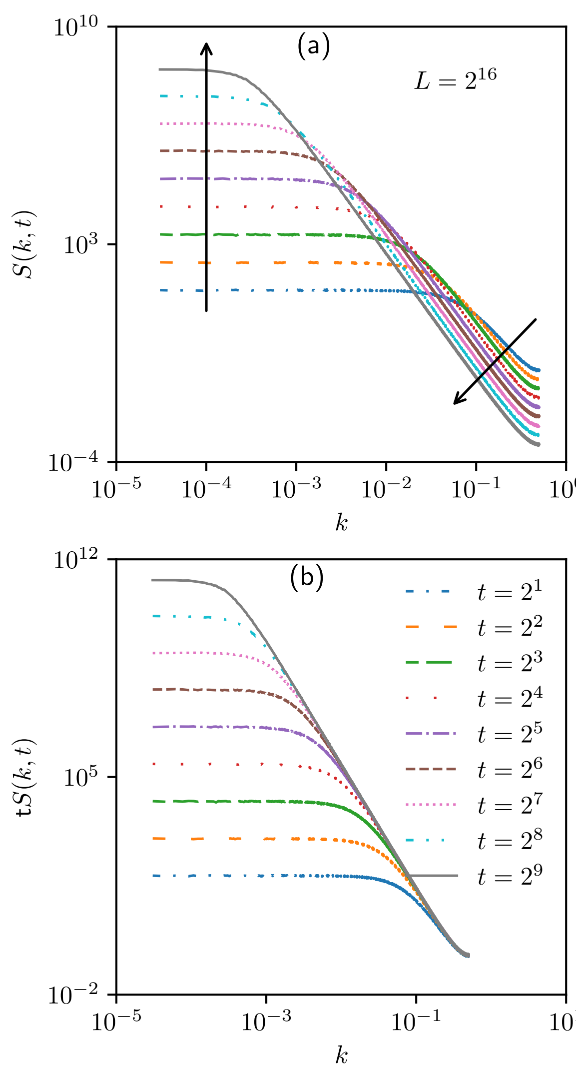

FIG. 3. For the Sneppen model. (a) The structure factor $S(k, t)$ after an evolution time t (in monolayers) for the rough profile $h(x, t)$, with $L = 2^{16}$. The arrows mark the effect of increasing growth time. (b) A clean plot of $tS(k, t)$ versus k shows the absence of time dependence in the nontrivial k regime, or $S(k, t) \sim 1/t$.

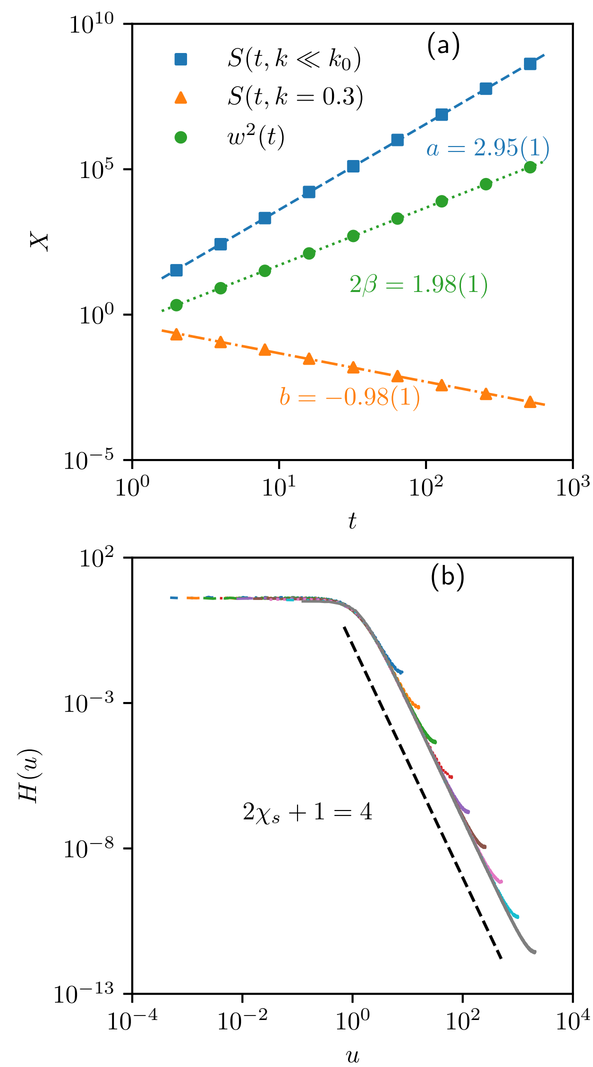

FIG. 4. In the Sneppen model. (a) At a fixed wave number k, the time scaling of power (■) $\sim t^a$ for $k \ll k_0$ and the power (▲) $\sim t^b$ for $k \gg k_0$. The symbol (●) corresponds to the square of the global width Â $w^2(t) \sim t^{2\beta}$. Straight lines are the best-fit curves. (b) The scaling function for the structure factor $H(u) \sim t^{-a} S(k, t)$, with an argument $u \sim kt^{1/z}$. We show data collapse using theoretically expected values for the two critical exponents $a = 3$ and $2\beta = 2$. Here, the typical characteristic exponents are $z = 1$, $\chi = 1$, and $\chi_s = 3/2$.

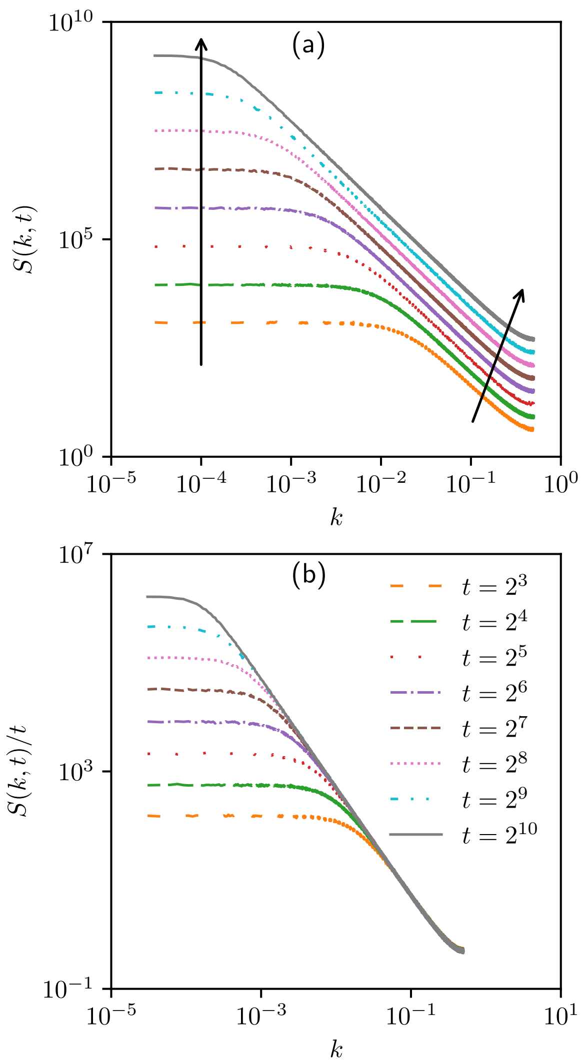

FIG. 5. Same as Fig. 3 for the anisotropic Sneppen model.

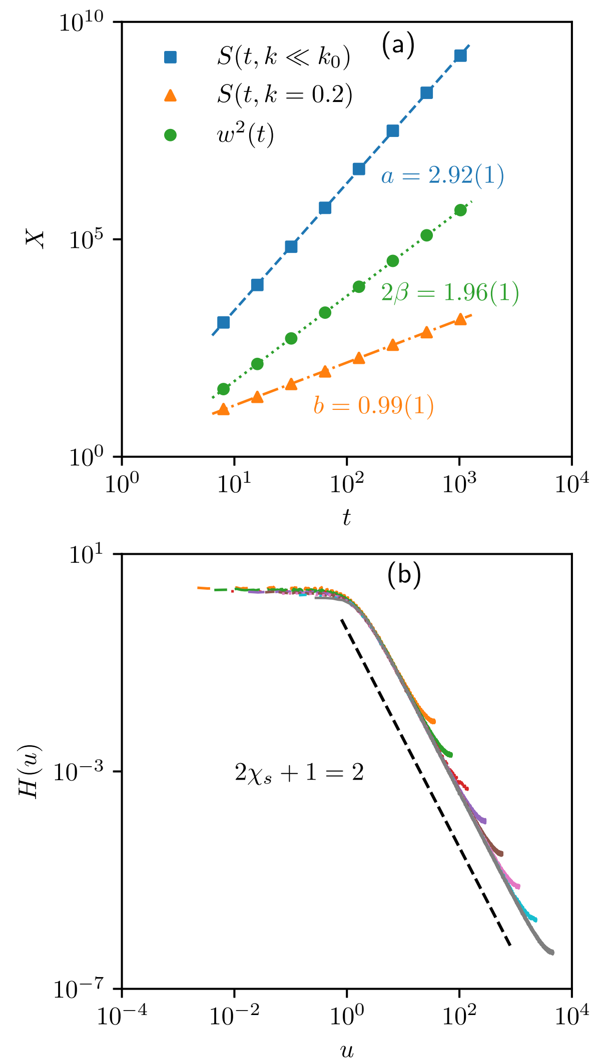

FIG. 6. Same as Fig. 4 for the anisotropic Sneppen model. Here, $z = 1$, $\chi = 1$, and $\chi_s = 1/2$.

which one can get from

$$\partial_t h = c\partial_x^3 h + (\partial_x h)^2/2 + \eta(x, t), \tag{11}$$

with $u = \partial_x h$. Here, c is a parameter. Interestingly, they observed that the height profile corresponding to the stochastic KdV equation also belongs to the same universality class as that of the tKPZ equation in one dimension. Similarly, the stochastic KdV equation and the inviscid stochastic Burger equation belong to the same universality. Our results suggest that the anisotropic Sneppen model and the tKPZ equation seem to share the same universality class.

For the MZB-2 model, the expected exponents, as mentioned in Ref. [45] are $z = 1$ and $\chi = 1/2$. However, our numerical result (not shown) suggests ($\chi_s = \chi < 1$), with $z \approx 0.6$ and $\chi \approx 1/2$.

Figure 7 shows the scaling function for the global interface width $w(t, L)$ for both dynamical rules of the Sneppen model. We find that $w(t, L)$ behaves exactly in the same manner for both models, with $z = 1$ and $\chi = 1$. However, the global interface width is not able to capture the anomalous features, despite the fact that the models belong to different universality classes.

V. CONCLUSION

We employed both finite-size and finite-time scaling methods for examining the dynamical structure factor of anomalous rough interfaces. We emphasized that the method can accurately determine the *universality features* (the critical exponents and the scaling functions). In particular, we applied the methods to a class of discrete models (the Seppen model and the Maslov-Zhang model) of rough interfaces in the presence of quenched disorder driven by extremal dynamics. Interestingly, the finite-size scaling analysis reveals the structure factor remains independent of system size for fixed growth times (in monolayers). This also offers an alternative way to characterize the anomalous rough interfaces.

Finally, we emphasize the system-specific findings of our simulation studies. (i) The MZB-1 model shows faceted patterns ($\chi_s > \chi$), with $z = 1$, $\chi = 1$, and $\chi_s = 3/2$. Strikingly, the model belongs to the same universality class as that of the Sneppen model. (ii) We also introduced an anisotropic variant of the Sneppen model. The model shows an intrinsically anomalous feature ($\chi_s < \chi$), with $z = 1$, $\chi = 1$, and

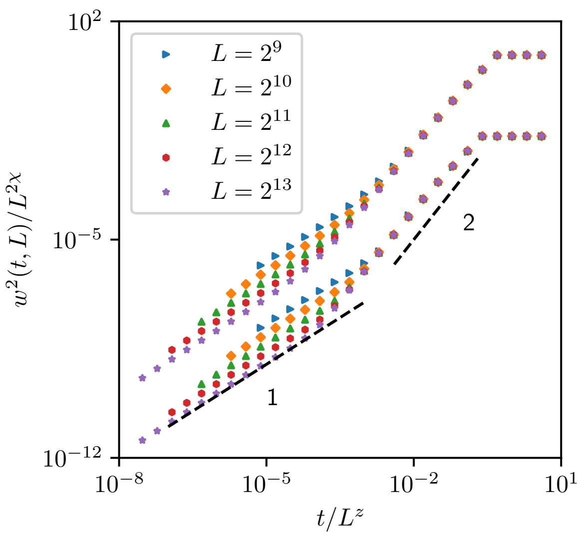

FIG. 7. Data collapse of the squared global interface width for the Sneppen model, with $z = 1$ and $\chi = 1$. The three regimes, namely, the random deposition growth $t \ll 1$, the nonlinear growth regime $1 \ll t \ll L^z$, and the saturation regime $t \gg L^z$ are clearly distinguishable. The time is measured in monolayers. The lower (upper) curves belong to isotropic (anisotropic) dynamics.

$\chi_s = 1/2$, and seems to belong to the tKPZ class or the height profile corresponding to the stochastic KdV equation [46]. (iii) In particular, the MZB-2 model has been of interest in the context of a solvable model of self-organized criticality (SOC) [45]. Although the MZB-2 model exhibits Family-Vicsek scaling ($\chi = \chi_s < 1$) with $z \approx 0.6$ and $\chi \approx 1/2$, the dynamical exponent significantly differs from the previously argued value $z = 1$ [45]. Therefore, the MZB-2 model does not belong to the same universality class as the SOC model discussed in Ref. [45]. We also examined several discrete models of the standard universality classes and consistently found the applicability of the FSS and FTS methods. In fact, the approach is general and applicable to a wide range of rough surfaces or interfaces. Although the methods can enhance our understanding significantly, the entire set of physical features that determine anomalous behavior needs further exploration.

Córdoba-Torres *et al*. experimentally studied the kinetic roughening of dissolving polycrystalline pure iron and found that the surface images exhibit two growth regimes [54]. In regime I, which has initial dissolution charges up to 4.5 C, the metal surface displays an intrinsic anomalous roughening. Regime II corresponds to the thick film limit, and the metal surface has a high morphological anisotropy. In regime II, one-dimensional interfaces along the orthogonal direction to the anisotropy show anomalous roughening with faceted features [54].

It is well known that the KPZ equation remains invariant under Galilean transformation, yielding a scaling relation $\chi + z = 2$ [2]. The same relationship seems to hold for the Sneppen model (cf. Table I). However, the space inversion symmetry $x \to -x$ is broken in the anisotropic Sneppen model [cf. Fig. 1(b)], and the same happens for the height process for the KdV equation because of an odd derivative term in space [cf. Eq. (11)]. Since the height process for the KdV equation belongs to the tKPZ universality class [46], the class should not respect the space inversion symmetry. However, this is unclear from Eq. (10). We infer that although the anisotropic Sneppen model has quenched noise and the tKPZ class has Gaussian noise, both have some common features: large nonlinearity, the scaling relation $\chi + z = 2$, and possibly a lack of space-inversion symmetry.

Importantly, only two exponents are independent for the models studied here. For the Sneppen model and MZB-1, $\chi + z = 2$ implies that z and χ_s are independent exponents. Although the MZB-2 model does not follow the scaling relation, there are two independent exponents, z and χ, as $\chi_s = \chi$.

ACKNOWLEDGMENTS

R.C. acknowledges financial support through the Junior Research Fellowship, UGC, India. A.C.Y. acknowledges a seed grant under IoE by Banaras Hindu University (Seed Grant No. II/2022-23/48729). We also acknowledge that the paper has been greatly enhanced by the comments of anonymous referees.

[1] T. Halpin-Healy and Y.-C. Zhang, Phys. Rep. **254**, 215 (1995).
[2] A.-L. Barabási and H. E. Stanley, *Fractal Concepts in Surface Growth* (Cambridge University Press, Cambridge, England, 1995).
[3] U. C. Täuber, *Critical Dynamics: A Field Theory Approach to Equilibrium and Non-Equilibrium Scaling Behavior* (Cambridge University Press, Cambridge, England, 2014).
[4] F. L. Forgerini and R. Marchiori, Biomatter **4**, e28871 (2014).
[5] J. Soriano, J. J. Ramasco, M. A. Rodríguez, A. Hernández-Machado, and J. Ortín, Phys. Rev. Lett. **89**, 026102 (2002).
[6] J. M. López and J. Schmittbuhl, Phys. Rev. E **57**, 6405 (1998).
[7] L. Ponson, D. Bonamy, and E. Bouchaud, Phys. Rev. Lett. **96**, 035506 (2006).
[8] J. M. López and H. J. Jensen, Phys. Rev. Lett. **81**, 1734 (1998).
[9] S. Das Sarma and P. Tamborenea, Phys. Rev. Lett. **66**, 325 (1991).
[10] Z.-W. Lai and S. Das Sarma, Phys. Rev. Lett. **66**, 2348 (1991).
[11] J. M. Kim and S. Das Sarma, Phys. Rev. Lett. **72**, 2903 (1994).
[12] S. F. Edwards and D. R. Wilkinson, Proc. R. Soc. London A **381**, 17 (1982).
[13] M. Kardar, G. Parisi, and Y.-C. Zhang, Phys. Rev. Lett. **56**, 889 (1986).
[14] T. Sasamoto and H. Spohn, Phys. Rev. Lett. **104**, 230602 (2010).
[15] P. Calabrese and P. Le Doussal, Phys. Rev. Lett. **106**, 250603 (2011).
[16] K. A. Takeuchi, Physica A **504**, 77 (2018).
[17] D. Squizzato and L. Canet, Phys. Rev. E **100**, 062143 (2019).

[18] K. Deligiannis, Q. Fontaine, D. Squizzato, M. Richard, S. Ravets, J. Bloch, A. Minguzzi, and L. Canet, Phys. Rev. Res. **4**, 043207 (2022).
[19] R. Gutiérrez and R. Cuerno, Phys. Rev. Res. **5**, 023047 (2023).
[20] F. Family, J. Phys. A: Math. Gen. **19**, L441 (1986).
[21] W. Kwak and J. M. Kim, Physica A **520**, 87 (2019).
[22] M. Eden, *Symposium on Information Theory in Biology* (Pergamon, New York, 1958).
[23] F. Family and T. Vicsek, J. Phys. A: Math. Gen. **18**, L75 (1985).
[24] J. M. Kim and J. M. Kosterlitz, Phys. Rev. Lett. **62**, 2289 (1989).
[25] K. A. Takeuchi and M. Sano, Phys. Rev. Lett. **104**, 230601 (2010).
[26] K. A. Takeuchi, M. Sano, T. Sasamoto, and H. Spohn, Sci. Rep. **1**, 34 (2011).
[27] S. Najem, A. Krayem, T. Ala-Nissila, and M. Grant, Phys. Rev. E **101**, 050301(R) (2020).
[28] K. Fujimoto, R. Hamazaki, and Y. Kawaguchi, Phys. Rev. Lett. **124**, 210604 (2020).
[29] G. Foltin, K. Oerding, Z. Rácz, R. L. Workman, and R. K. P. Zia, Phys. Rev. E **50**, R639 (1994).
[30] S. Raychaudhuri, M. Cranston, C. Przybyla, and Y. Shapir, Phys. Rev. Lett. **87**, 136101 (2001).
[31] Z. Toroczkai, G. Korniss, S. Das Sarma, and R. K. P. Zia, Phys. Rev. E **62**, 276 (2000).
[32] Y. Shapir, S. Raychaudhuri, D. G. Foster, and J. Jorne, Phys. Rev. Lett. **84**, 3029 (2000).
[33] Z.-P. Xun, J.-X. Li, Y. Jiao, R.-T. Li, and G. Tang, Physica A **540**, 122998 (2020).
[34] J. M. López, Phys. Rev. Lett. **83**, 4594 (1999).
[35] J. J. Ramasco, J. M. López, and M. A. Rodríguez, Phys. Rev. Lett. **84**, 2199 (2000).
[36] J. M. López and M. A. Rodríguez, Phys. Rev. E **54**, R2189 (1996).
[37] J. M. López, M. A. Rodríguez, and R. Cuerno, Physica A **246**, 329 (1997).
[38] J. M. López, M. Castro, and R. Gallego, Phys. Rev. Lett. **94**, 166103 (2005).
[39] I. G. Szendro, J. M. López, and M. A. Rodríguez, Phys. Rev. E **76**, 011603 (2007).
[40] A. Alés and J. M. López, Phys. Rev. E **99**, 062139 (2019).
[41] A. Alés and J. M. López, J. Stat. Mech.: Theory Exp. (2020) 033210.
[42] A. Alés and J. M. López, Phys. Rev. E **104**, 044108 (2021).
[43] V. H. Purrello, J. L. Iguain, and A. B. Kolton, Phys. Rev. E **99**, 032105 (2019).
[44] K. Sneppen, Phys. Rev. Lett. **69**, 3539 (1992).
[45] S. Maslov and Y.-C. Zhang, Phys. Rev. Lett. **75**, 1550 (1995).
[46] E. Rodríguez-Fernández, S. N. Santalla, M. Castro, and R. Cuerno, Phys. Rev. E **106**, 024802 (2022).
[47] C. Cartes, E. Tirapegui, R. Pandit, and M. Brachet, Philos. Trans. R. Soc. London A **380**, 20210090 (2022).
[48] C. Fontaine, F. Vercesi, M. Brachet, and L. Canet, Phys. Rev. Lett. **131**, 247101 (2023).
[49] S. Zaitsev, Physica A **189**, 411 (1992).
[50] P. Meakin, P. Ramanlal, L. M. Sander, and R. C. Ball, Phys. Rev. A **34**, 5091 (1986).
[51] E. Daryaei, Phys. Rev. E **101**, 062108 (2020).
[52] M. Plischke, Z. Rácz, and D. Liu, Phys. Rev. B **35**, 3485 (1987).
[53] B. Derrida, Phys. Rep. **301**, 65 (1998).
[54] P. Córdoba-Torres, T. J. Mesquita, I. N. Bastos, and R. P. Nogueira, Phys. Rev. Lett. **102**, 055504 (2009).